Hindawi
Shock and Vibration
Volume 2018, Article ID 6563537, 10 pages
https://doi.org/10.1155/2018/6563537

Research Article

Crack Detection of Reinforced Concrete Structures Based on BOFDA and FBG Sensors

Qinghua Zhang[1,2,3] and Ziming Xiong[1,2]

[1]*College of Mechanical Engineering, Nanjing University of Science and Technology, Nanjing, Jiangsu 210094, China*
[2]*State Key Laboratory of Disaster Prevention and Mitigation of Explosion and Impact, Army Engineering University of PLA, Nanjing, Jiangsu 210007, China*
[3]*State Key Laboratory of Geo-information Engineering, Xian, Shannxi 710054, China*

Correspondence should be addressed to Ziming Xiong; xzm992311@163.com

Received 24 May 2018; Revised 15 July 2018; Accepted 29 July 2018; Published 3 September 2018

Academic Editor: Daniele Baraldi

Reinforced concrete structural elements, as an important component of buildings and structures, require inspection for the purposes of crack detection which is an important part of structural health monitoring. Now existing crack detection methods usually use a single technology and can only detect internal or external cracks. In this paper, the authors propose a new sensing system combining BOFDA (Brillouin optical frequency-domain analysis) and FBG (fiber Bragg grating) technology, which are used to detect internal and surface cracks and their development in reinforced concrete structures, and an attempt is made to estimate the width of surface cracks. In these experiments, a special reinforced concrete beam structure was designed by the author for crack detection under load. Four continuous distributed optical fibers are fixed on the steel skeleton, which is located within the reinforced concrete beam. Three FBG sensors are fixed on the lower surface of the beam, near its centre. By analysing the sensor data, it can be found that the BOFDA-distributed fiber can be used to detect internal cracking before surface cracking, and the difference between scans can be used to judge the time of onset of internal cracking, but the relative error in position is about 5%, while the FBG sensor can detect the cracking time of microcracks on the lower surface in near-real-time and can be used to calculate the crack width. Through the experiment, it is found that if the combination of BOFDA and FBG technology is adopted, we can initially use the strain data obtained by multiple groups of BOFDA monitoring to predict the general location of the internal cracks, then to monitor the exact location of the surface cracks by FBG in the medium term, and to estimate the width of the final expansion of the cracks finally.

1. Introduction

Reinforced concrete structures are widely used [1, 2] due to load and other mechanical factors, and the concrete structure may crack [3, 4]. These cracks may develop into large cracks that can pose a threat to the safety of the structure with time, so it is necessary to monitor the cracks [5–7]. There are two types of cracks in reinforced concrete beams, surface cracks [8, 9] and internal cracks [10–12]. When the crack occurs inside the beam, it gradually develops and internal cracks penetrate the surface cracks, which results in structural damage. The two cracks often form cracks inside and outside the structure. For the monitoring of cracks in reinforced concrete structures, traditional methods include identification from visual images [13–15], resistance strain gauges [16], the ultrasonic rebound method [17, 18], and the X-ray CT method [19, 20]; however, due to the influence of external environmental factors, the cracking of a reinforced concrete structure is often random. The above methods require manual assistance and suffer from hysteresis and thus cannot realise long-term, real-time, extensive monitoring.

The use of optical fiber sensing for crack detection is a new technology developed in recent years. It has the advantages of real-time monitoring, dynamic data logging, and high precision. Optical fiber sensing technology can be

divided into two types: distributed and point [21–23]. Distributed optical fiber sensing technology for crack monitoring includes OTDR (optical time-domain reflectometer) [24, 25], BOTDR (Brillouin optical time-domain reflectometer) [26, 27], BOTDA (Brillouin optical time-domain analysis) [28–30], BOFDA (Brillouin optical frequency-domain analysis) [31], and BOCDA (Brillouin optical correlation-domain analysis) [32]. They can allow continuous monitoring, but their accuracy is low. The point-based fiber optic sensors used in crack monitoring are mainly FBG technology, and a large number of FBG sensors are used for crack monitoring in concrete structures [33–38]. Zaidi and Krebber proposed a BOFDA/FBG sensor system for simultaneous temperature/strain measurements [39], which provides inspiration for the integration of BOFDA and FBG for monitoring internal and external cracks. However, there is little reported research on the monitoring of cracks in reinforced concrete structures using a combination of distributed (BOFDA) and point (FBG) methods. BOFDA is a distributed technology which can detect the location of cracks in the whole optical fiber area but has low spatial resolution. In contrast, FBG has a high position measurement precision, and it should be placed in a critical stress location to compensate for the lack of spatial resolution of BOFDA. The authors will try to use both BOFDA and FBG techniques to monitor the cracks at the same time in this paper.

This paper is organised as follows: in Section 2, the principles of BOFDA sensing and FBG sensing technology are described briefly; in Section 3, the experimental setup is introduced, including the design of a reinforced concrete beam and the fixing of BOFDA and FBG sensors thereon; in Section 4, an analysis of BOFDA and FBG experimental data is presented; and in Section 5, the conclusions are summarised.

2. Sensing Principle of BOFDA and FBG

2.1. BOFDA. BOFDA (Brillouin optical frequency-domain analysis) technology is proposed by Garus et al. and enshrines the basic principles of BOFDA technology, as well as using pulsed light and probe lighting [40]. Relationships between temperature, strain, and Brillouin optical frequency drift were used to obtain the information of each measurement point on the fiber:

$$\nu_B(\varepsilon,\ T)\,\frac{d\nu_B(T)}{dT}\left(T-T_0\right)=\nu_B(0)+\frac{d\nu_B(\varepsilon)}{d\varepsilon}\varepsilon, \tag{1}$$

where $\nu_B(0)$ is the Brillouin frequency shift in the initial state, $\nu_B(\varepsilon,\ T)$ is the Brillouin frequency shift at any time, $(d\nu_B(T))/dT$ is the temperature term, $(d\nu_B(\varepsilon))/d\varepsilon$ is the strain term, $(T-T_0)$ is the temperature change, and ε is the change in strain. When the temperature effect is ignored, Equation (1) is simplified to

$$\nu_B(\varepsilon)=\nu_B(0)+\frac{d\nu_B(\varepsilon)}{d\varepsilon}\varepsilon. \tag{2}$$

The following formula can be derived from Formula (2):

$$\frac{\varepsilon}{d\varepsilon}=\frac{\nu_B(\varepsilon)-\nu_B(0)}{d\nu_B(\varepsilon)}. \tag{3}$$

The expression of strain ε can be obtained from Formula (3), and it is also the key variable to crack detection:

$$\varepsilon=-\frac{\Delta\nu_B}{\overline{\nu}_B*\mathrm{Ks}}, \tag{4}$$

where $\overline{\nu}_B$ is the average frequency, Ks = 0.78. When internal cracks are not easy to find, time series data of strain are used to detect cracks. In the case where the value of the data sequence is abrupt (usually the spike), it is determined that the location of the crack occurs. In addition, it can be verified by the location of the external cracks.

2.2. FBG. A fiber Bragg grating (FBG) is a passive optical component in an optical fiber, which is one of the most widely used optical fiber sensors. This sensor can change the wavelength of the reflected light according to the change in temperature or strain. The basic principle of strain sensing in a FBG sensor is shown in Figure 1.

When a beam of light is propagated in the fiber Bragg grating, each segment of the fiber will only reflect a specific wavelength of light, and the wavelength is called the Bragg wavelength after the refractive index is changed (Equation (5)). The wavelength of the signal reflected by the Bragg grating is [41, 42]

$$\lambda_B=2n_{\mathrm{eff}}\Lambda, \tag{5}$$

where n_{eff} is the effective refractive index of the fiber core and Λ is the grating period and is the mode index or effective refractive index of the fiber, which can be regulated by changing the relative angle between two interference ultraviolet beams to produce various wavelength-tuned gratings.

λ_B also is the central wavelength of the reflected signal, which is influenced by n_{eff} and Λ. Moreover, the central reflection wavelength is strain- and temperature-dependent; according to the principle illustrated above, the relationship of reflection wavelength and measured parameters can be established. The relationship between reflection wavelength $\Delta\lambda$ and longitudinal strain $\Delta\varepsilon$ is given by [43, 44]

$$\frac{\Delta\lambda_B}{\lambda_B}=\left(1-P_e\right)\Delta\varepsilon, \tag{6}$$

where $P_e=-((1/n)(dn/d\varepsilon))$ is the strain optical coefficient. From Formula (4), we can get the following expression of strain:

$$\varepsilon=\frac{\Delta\lambda_B}{\lambda_B\left(1-P_e\right)}+\varepsilon_0. \tag{7}$$

The strain of the crack FBG pasted region can be calculated by the change of the internal wavelength of the fiber, such as Formula (7), where ε_0 is the initial strain. Similar to BOFDA's method of crack detection analysis, the locations of cracks are determined by the location of abrupt changes in time series (step in the data).

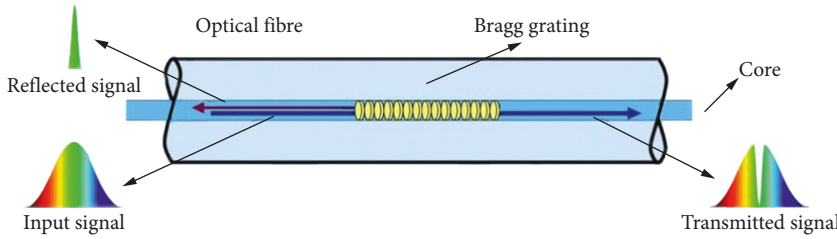

Figure 1: Working mechanism of an FBG sensor.

3. Experimental Work

3.1. The Design of a Reinforced Concrete Beam. The laboratory conditions make it difficult to do a full-scale concrete beam loading test: if the beam weighs too much, it will affect the test, and if it is too long or too small, it is difficult to meet test accuracy requirements, so the test beam parameters are designed as shown in Table 1.

Reinforcement of reinforced concrete beams is done as shown in Figure 2; ① is the longitudinal reinforcement, ② is the tensile tendons (diameter 10 mm), and ③ is the double hoop (diameter 8 mm and spacing 50 mm); the ultimate load is 37.39 kN.

Figure 3(a) shows the loading form of reinforced concrete beams, and the deformation of which is shown in Figure 3(b). Figures 3(c) and 3(d) show the bending moment and shear force diagrams under concentrated load, respectively. The bending moment and shear force in the cross section are the largest, which is the location where the first crack occurs under load.

3.2. Fixing Method: BOFDA and FBG Sensors. To monitor internal and surface cracks in the reinforced concrete beam, fiber optic sensors and FBG sensors are simultaneously fixed in its interior and surface. Figure 4 shows the layout of the fiber optic sensor and the FBG sensor, and the specific surface and internal embedding fix process and method consists of four steps as follows.

In the first step, an optical fiber sensor is fixed inside the reinforced concrete beam, which will be used for internal crack monitoring based on BOFDA technology. As shown in Figure 5(a), before the concrete beam is poured, it is necessary to fix the encapsulated optical fiber to the reinforcing cage by strapping. The fiber in the concrete beam is used in the four back-and-forth loops of the circuit layout: the concrete pouring then takes place (Figure 5(b)). It should be noted that the concrete pouring process had to be done to fix the sensor, and in particular, we pay attention to the direction of connection of the fiber to avoid bending and damage.

In the second step, we fixed the FBG sensors on the lower surface of the concrete beam. To improve the strain transfer rate and monitor the crack efficiency, bare FBG sensors are used in this experiment (Figure 6(a)). Before fixing the FBG sensors, the lower surface of the concrete beam is polished smooth using a grinder. After this, alcohol is used to clean the surface, and epoxy resin is used to fill the surface voids after drying. After 24 hours, the FBG sensor was fixed to the lower surface of the concrete beam with 502 glue (Figure 6(b)).

In the third step, instruments are used for data collection. The BOFDA demodulator is used to obtain distributed fiber centre frequency changes and then record the strain information at the measurement point (Figure 7(a)). The wavelength change of the FBG sensors is collected by using a MOI SM-125 demodulator with a scanning frequency of 2 Hz (Figure 7(b)).

The fourth step entails the loading experiment: the concrete beam is placed on the reaction frame, the left and right sides are supported, and the jack is positioned. The 100 kN load cell is housed between the jack and the reaction stand to measure the load during the test. The load cell data contain a strain gauge (Figure 8).

4. Results

4.1. Data Analysis: BOFDA Sensors and FBG Sensors. By analysing the loading mode of the reinforced concrete beam, the position of maximum strain can be calculated and forms the earliest location of cracking (using finite element analysis and the results in Figures 3(a)–3(d)). Correspondingly, the theoretical positions on the fiber are 7.55 m, 11.90 m, 15.55 m, and 19.60 m. Inside the concrete beam, the distributed fiber is arranged in an S shape, and the four positions correspond to the same possible cracking positions. The concrete beam was scanned 13 times (100 seconds) using BOFDA technology. The results show that the strain measurement curve has four peak points (Figure 9). Among them, the first peak point position approximates to the loaded section of the beam, which is in good agreement with the theoretical value, while the other three peaks are influenced by the spatial resolution, and there are some errors therein. The mean values of the four peak positions are 7.55 m, 11.25 m, 14.95 m, and 18.65 m, and the statistical and error data pertaining thereto are listed in Table 2.

The relative error in the actual measurement position is between 5.8% and 10%, within ideal range, but for the 2.2 m long concrete beam, the error is slightly larger; however, it is difficult to determine the time when cracking occurs only according to the results in Figure 9. As shown in Figure 10, the strain time series from BOFDA scanning are subjected to differential time series effects. Figure 10 shows that three independent spikes appear in the 3rd graph (T4-T3), but from the 4th graph (T5-T4) to the 12th graph (T13-T12), four distinct spikes can be found in almost the same position. When the small cracks on the lower surface of the

Table 1: Reinforced concrete beam design.

Size (mm)	Concrete grade	Longitudinal bar	Stirrups	Thickness of the protective layer (mm)
180 × 250 × 2200	C35	HRB400	HPB300	25

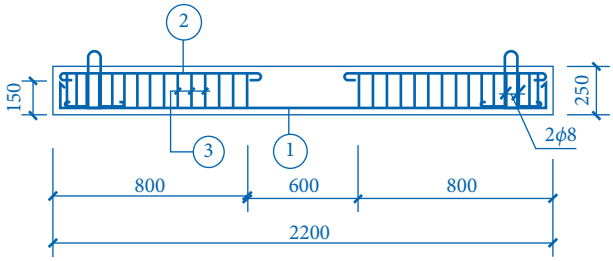

Figure 2: Reinforcement of reinforced concrete beams.

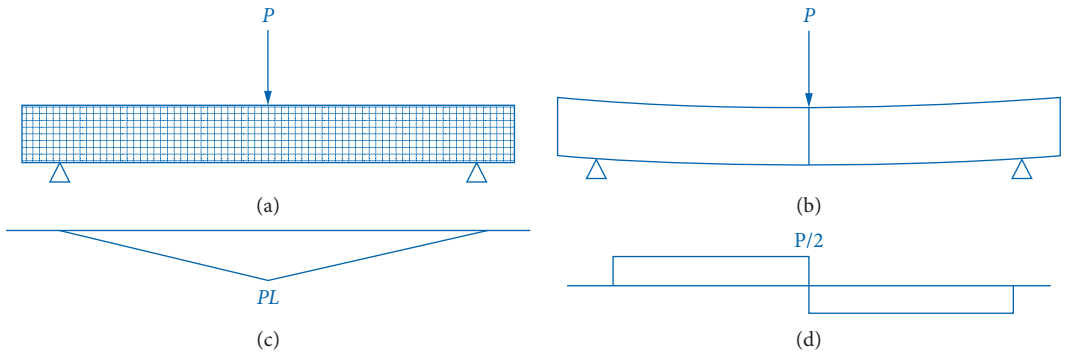

Figure 3: (a) Schematic diagram of loading of reinforced concrete beams. (b) Schematic diagram of loading and unloading of reinforced concrete beams. (c) Bending moment diagram. (d) Shear force diagram.

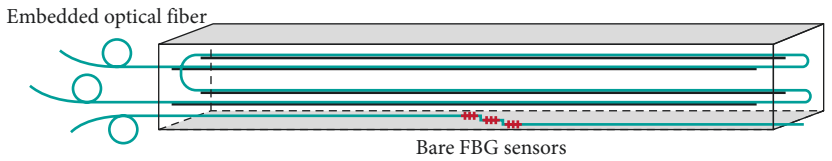

Figure 4: The sensor positions.

(a) (b)

Figure 5: Layout of fiber optic sensors. (a) Installation of fiber optic sensors on the beam. (b) Poured concrete beams.

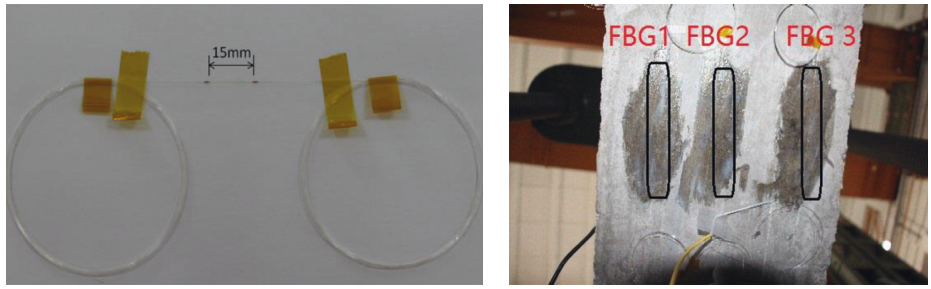

(a) (b)

Figure 6: Fixing FBG sensors. (a) Bare FBG sensor. (b) Pasting of FBG sensors.

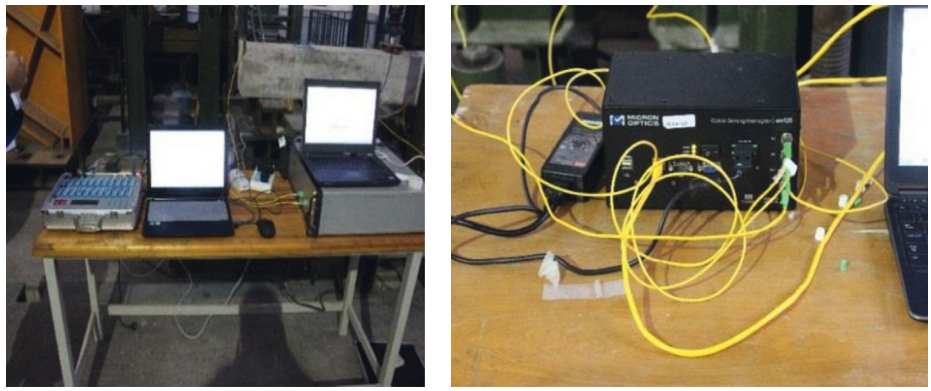

(a) (b)

Figure 7: Data acquisition instruments. (a) BOFDA device. (b) SM-125 demodulator.

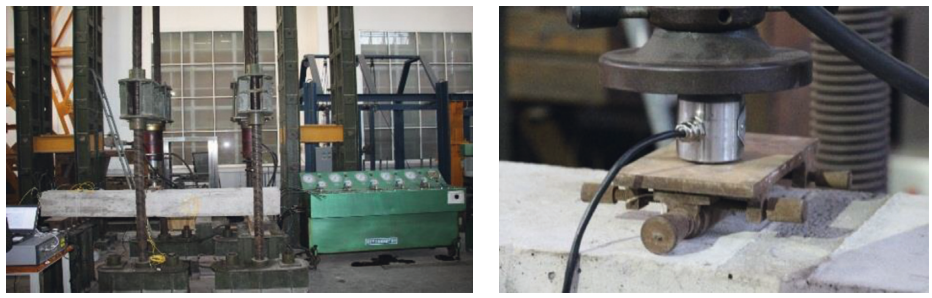

(a) (b)

Figure 8: Test loading process.

concrete are found, that time corresponds to the time period of the fourth graph (T5-T4) in Figure 10; since the fiber optic sensor is fixed inside the concrete beam, the time at which the internal crack occurs is based on the third graph (T4-T3) according to the differential time series of Figure 10 and the time at which the surface crack occurs. The 3rd graph (T4-T3) shows the moment when the fracture first occurred, and from the 4th graph (T5-T4) to the 12th graph (T13-T12), four distinct peaks can be found in almost the same position. When the 4th to 12th graphs show gradual crack expansion, in the 12th graph, the increase in strain at the peak is close to 1000 microstrain. Moreover, the strain around the crack is significantly increased.

The three bare FBG sensors are located at the bottom of the concrete beam (Figure 11) with their central wavelengths of 1584 nm, 1560 nm, and 1550 nm, respectively. During the step-by-step loading of the loader, the stepped strain monitoring graph is obtained from three FBG sensors, as shown in Figure 12. Among them, the strain time series of FBG1 and FBG2 are similar, but FBG3 is above other two. The author concluded that cracks were generated in the paste gauge of FBG3 sensor. In fact, the first crack was found in the

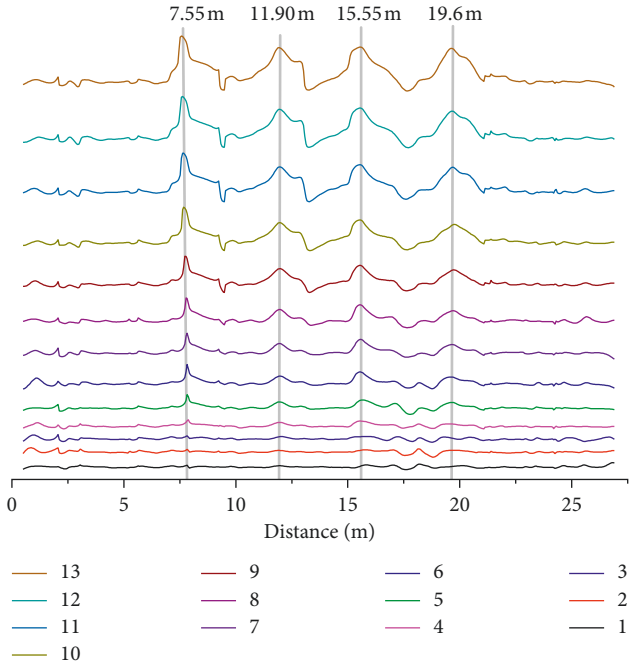

Figure 9: Results of 13 scans using BOFDA.

Table 2: Error statistic.

Theoretical position (m)	Measured position (m)	Relative error (%)
7.55	7.55	0
11.25	11.90	5.8
14.95	15.55	4.0
18.65	19.6	5.1

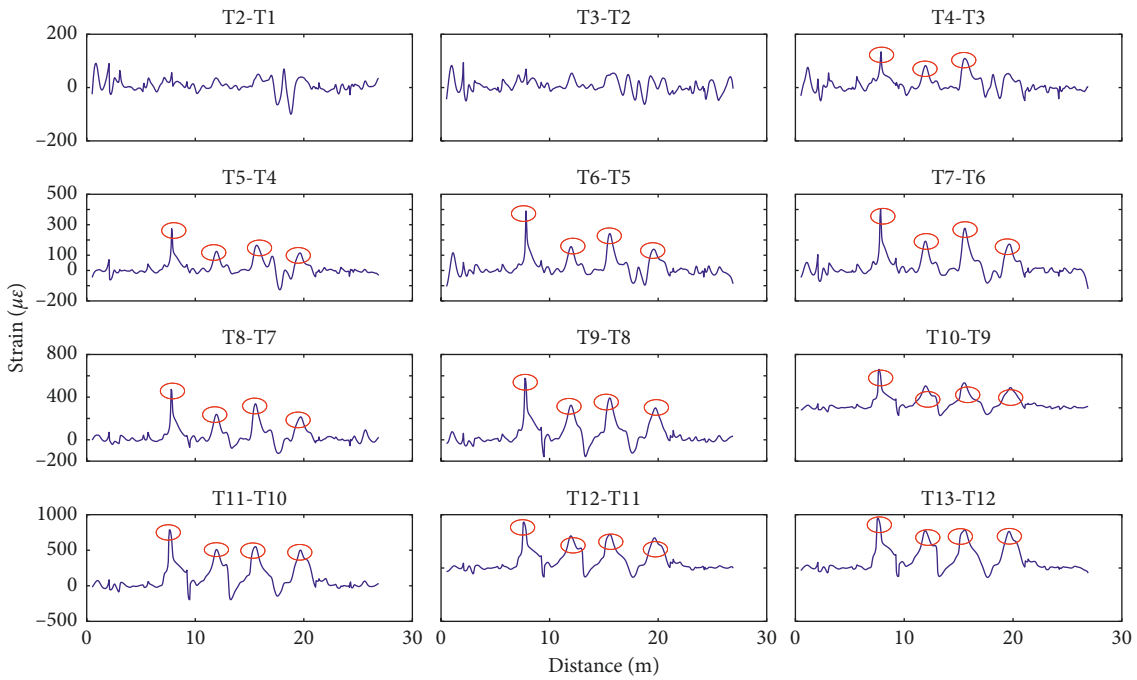

Figure 10: Differential time series data: BOFDA scanning.

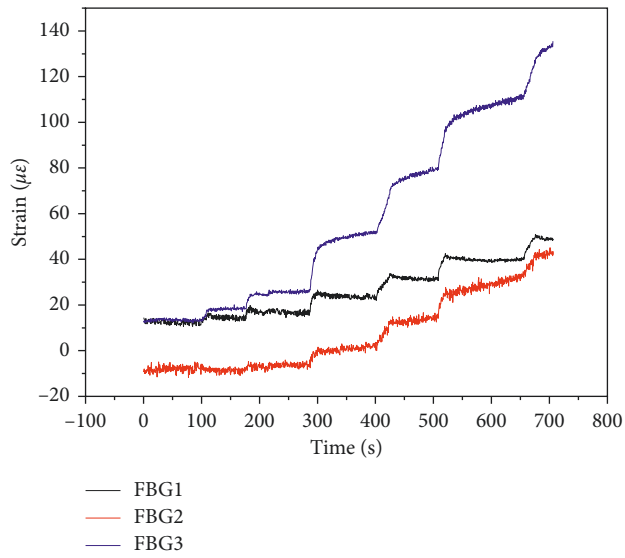

Figure 11: (a) First-order difference time series. (b) AR (3) smoothing sequence of FBG 3 sensor.

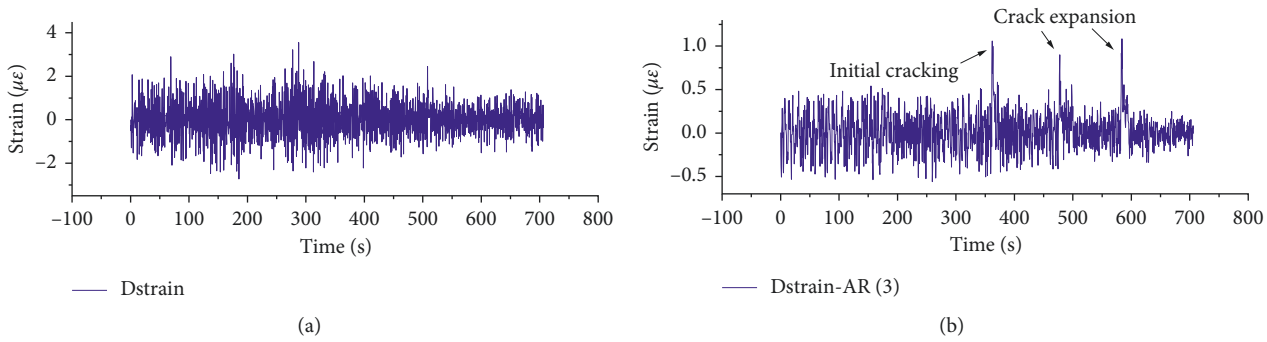

Figure 12: Strain time series: three FBG sensors.

area by eye, and at the same time, no cracks were found in the paste gauge of FBG1 and FBG2 sensors. It can be concluded that the bare fiber grating sensor can effectively monitor the occurrence of cracks.

According to several FBG strain time series, the location of the crack can be roughly determined; however, the time to onset of cracking is almost impossible to determine. To find the time when the crack occurs, the strain data of the FBG3 sensor are subjected to first-order differential analysis (dstrain in Figure 11(a)), but it is almost impossible to determine the time with sufficient precision due to oversampling of the data. In the next analysis, the AR (3) model is used to smooth the first-order differential sequence. The notation AR (p) indicates an autoregressive model of order p. In this paper, the AR (3) model is defined as

$$\varepsilon_t = c + \sum_{i=1}^{3} \varphi_i \varepsilon_{t-i} + \delta_t, \tag{8}$$

where φ_i are the parameters of the model, c is a constant, and δ_t is the white noise. By analysing the AR (3) sequence (dstrain-AR (3) in Figure 11(b)), we found a significant data spike at 362 s, which is in good agreement with the moment of artificial recording of the initial cracking: the data jumps at 478 s and 584 s correspond to the rapid expansion of the crack.

4.2. Initial Estimation of the Crack Width. With fiber and FBG sensors, the position and timing of both internal and external cracks can be detected. Furthermore, the author attempted to use FBG data to estimate the crack width. In the experiment, the author attempted to estimate the width of crack 1 (red box, Figure 13) by using the strain data measured by the FBG 3 sensors. The crack widths were evaluated by high-precision fracture gauges.

The final crack width can be calculated using FBG data:

$$\begin{aligned} \varepsilon &= \frac{\Delta\lambda}{k\lambda}, \\ \varepsilon &= 2431.62\ \mu\varepsilon, \\ \omega &= \varepsilon l, \\ \omega &= 0.24\ \text{mm}, \end{aligned} \tag{9}$$

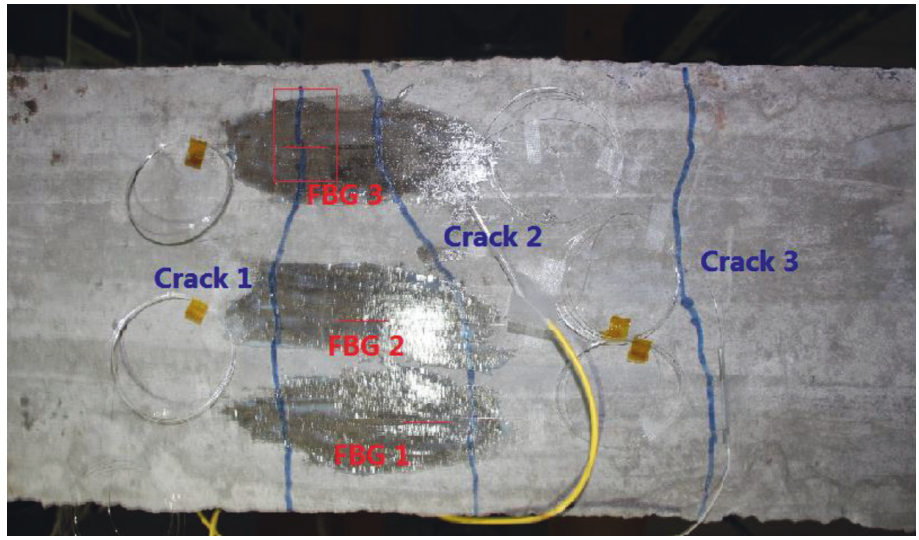

Figure 13: Cracking of the beam bottom.

(a) (b)

Figure 14: Visual crack width measurement. (a) KON-FK (B) crack width observation instrument. (b) Crack measurement.

where $\Delta\lambda$ is the value of the change in wavelength, the value of k is 0.78×10^{-6}, and the gauge length of the sensor is 100 mm (l).

To verify the calculated crack width as measured by the FBG sensor, a crack width observation instrument is used (Figure 14(a)). The crack width obtained from the crack width observation instrument was 0.16 mm, and the FBG measurement was 0.24 mm: a relative error of about 50% of the crack width was measured by FBG, but nevertheless, it is feasible to use FBG sensors to measure crack widths.

5. Conclusion

A reinforced concrete beam designed by the author is used in the paper, in which distributed fiber and FBG sensors are fixed inside and on the surface, respectively. The positions of these sensors are obtained from force analysis (including bending moment and shear force diagrams) of the beam during loading. Through the step-by-step loading of reinforced concrete beams, the information such as the cracking time, position, and width of internal and surface cracks are calculated according to the data collected using the sensors. Some conclusions can be obtained from these tests:

(1) The strain information pertaining to distributed fiber points can be measured by BOFDA technology, which can be used to detect the occurrence of internal cracks and external; however, due to the resolution of BOFDA technology, there are positional errors of less than 10% in the measurement of internal cracks.

(2) The bare FBG sensor is extremely sensitive and can monitor the surface strain and cracking of the concrete beam. It should be noted that the FBG sensor paste gauge need to cover the zone where cracks may occur. Otherwise, the FBG sensors may not detect the occurrence of cracking.

(3) The method of calculating the width of the crack using FBG strain monitoring data has a large error, which can monitor the width of the crack in real time; however, the reason for the low accuracy may be caused by factors such as strain transfer, temperature changes, and load vibration, which can be further improved in later experiments.

(4) If both the distributed fiber and the FBG sensor are used to monitor the cracks at the same time, the

appearance of the cracks inside and outside the concrete beam and the width of the surface cracks can be measured simultaneously. This scheme combines the advantages of BOFDA and FBG sensors, which would achieve better measurement results.

Data Availability

The data used in the paper are the firsthand data of the authors, and they are reliable. If the journal or readers need these data, the author can provide it after the publication of the paper.

Conflicts of Interest

The authors declare no conflict of interest.

Acknowledgments

This work was carried out under funding from the National Natural Science Foundation of China (Grant no. 41604024), China Postdoctoral Science Foundation (Grant no. 2016M601815), and the State Key Laboratory of Geoinformation Engineering (SKLGIE2016-Z-1-3).

References

[1] U. Dilek, "Assessment of fire damage to a reinforced concrete structure during construction," *Journal of Performance of Constructed Facilities*, vol. 21, no. 4, pp. 257–263, 2007.

[2] C. Zhao, J. Y. Chen, Y. Wang, and S. J. Lu, "Damage mechanism and response of reinforced concrete containment structure under internal blast loading," *Theoretical and Applied Fracture Mechanics*, vol. 61, pp. 12–20, 2012.

[3] A. P. Fantilli and B. Chiaia, "Golden ratio in the crack pattern of reinforced concrete structures," *Journal of Engineering Mechanics*, vol. 139, no. 9, pp. 1178–1184, 2013.

[4] S. J. Foster, B. Budiono, R. I. Gilbert et al., "Rotating crack finite element model for reinforced concrete structures," *Computers and Structures*, vol. 58, no. 1, pp. 43–50, 1996.

[5] Y. Theiner and G. Hofstetter, "Numerical prediction of crack propagation and crack widths in concrete structures," *Engineering Structures*, vol. 31, no. 8, pp. 1832–1840, 2009.

[6] Y. Fujita, Y. Mitani, Y. Hamamoto et al., "A method for crack detection on a concrete structure," in *Proceedings of International Conference On Pattern Recognition*, pp. 901–904, Cancun, Mexico, December 2006.

[7] B. Zhang, S. Wang, X. Li et al., "Crack width monitoring of concrete structures based on smart film," *Smart Materials and Structures*, vol. 23, no. 4, article 045031, 2014.

[8] P. Yeh and P. Liu, "Imaging of internal cracks in concrete structures using the surface rendering technique," *NDT and E International*, vol. 42, no. 3, pp. 181–187, 2009.

[9] H. Gao, Z. Ai, H. Yu et al., "Analysis of internal crack healing mechanism under rolling deformation," *PLoS One*, vol. 9, no. 7, Article ID e101907, 2014.

[10] K. Matsuyama, M. Yamada, and M. Ohtsu, "On-site measurement of delamination and surface crack in concrete structure by visualized NDT," *Construction and Building Materials*, vol. 24, no. 12, pp. 2381–2387, 2010.

[11] Y. C. Lin and W. C. Su, "Use of stress waves for determining the depth of surface-opening cracks in concrete structures," *NDT and E International*, vol. 30, no. 4, p. 255, 1997.

[12] H. G. Moon and J. H. Kim, "Intelligent crack detecting algorithm on the concrete crack image using neural network," in *Proceedings of the International Symposium on Automation and Robotics in Construction (ISARC 2011)*, Seoul, Republic of Korea, June-July 2011.

[13] Z. Zhu, S. German, I. Brilakis et al., "Visual retrieval of concrete crack properties for automated post-earthquake structural safety evaluation," *Automation in Construction*, vol. 20, no. 7, pp. 874–883, 2011.

[14] T. Su, "Application of computer vision to crack detection of concrete structure," *International Journal of Emerging Technologies in Learning*, vol. 5, no. 6, pp. 457–461, 2013.

[15] O. Buyukozturk, "Imaging of concrete structures," *NDT and E International*, vol. 31, no. 4, pp. 233–243, 1998.

[16] A. Lukashevich, V. A. Leonets, L. M. Chaus et al., "Strain-gauge method of detecting subcritical fatigue cracks in low-carbon steel welds," *Strength of Materials*, vol. 47, no. 3, pp. 467–473, 2015.

[17] W. Xu, J. Shen, C. Zhang et al., "Ultrasonic infrared thermal wave nondestructive evaluation for crack detection of several aerospace materials," in *Proceedings of Infrared Materials, Devices, and Applications (Photonics Asia 2007)*, vol. 6835, Beijing, China, 2007.

[18] P. Lasaygues, "Ultrasonic discrimination and modelling for crack-tip echoes," *Nondestructive Testing and Evaluation*, vol. 26, no. 1, pp. 67–85, 2010.

[19] W. Ren, Z. Yang, R. Sharma, C. Zhang, and P. J. Withers, "Two-dimensional X-ray CT image based meso-scale fracture modelling of concrete," *Engineering Fracture Mechanics*, vol. 133, pp. 24–39, 2015.

[20] I. S. Darma, T. Sugiyama, M. A. Promentilla et al., "Application of X-Ray CT to study diffusivity in cracked concrete through the observation of tracer transport," *Journal of Advanced Concrete Technology*, vol. 11, no. 10, pp. 266–281, 2013.

[21] C. K. Leung, N. Elvin, N. Olson, T. F. Morse, and Y. F. He, "Optical fiber crack sensor for concrete structures," in *Proceedings of Smart Structures and Materials 1997: Smart Sensing, Processing, and Instrumentation*, vol. 3042, San Diego, CA, USA, June 1997.

[22] H. Liu and Z. Yang, "Distributed optical fiber sensing of cracks in concrete," in *Proceedings of Optical and Fiber Optic Sensor Systems*, vol. 3555, Beijing, China, August 1998.

[23] T. Bao, J. Wang, and Y. Yao, "A fiber optic sensor for detecting and monitoring cracks in concrete structures," *Science China Technological Sciences*, vol. 53, no. 11, pp. 3045–3050, 2010.

[24] W. Zhang, J. Dai, H. Xu, B. Sun, and Y. Du, "Distributed fiber optic crack sensor for concrete structures," in *Proceedings of Advanced Sensor Systems and Applications III*, vol. 6830, Beijing, China, November 2007.

[25] J. Jang, S. Chang, N. Cho, and N. Kim, "Crack detection of structures using optical time domain reflectometry (OTDR) method," in *Proceedings of Smart Structures and Materials 2000: Smart Systems for Bridges, Structures, and Highways*, vol. 3988, pp. 276–283, Newport Beach, CA, USA, April 2000.

[26] A. Klar, Y. Goldfeld, and Z. Charas, "Measures for identifying cracks within reinforced concrete beams using BOTDR," in *Proceedings of Sensors and Smart Structures Technologies for Civil, Mechanical, and Aerospace Systems 2010*, vol. 7647, San Diego, CA, USA, March 2010.

[27] X. Feng, J. Zhou, C. Sun, X. Zhang, and F. Ansari, "Theoretical and experimental investigations into crack detection with

BOTDR-distributed fiber optic sensors," *Journal of Engineering Mechanics*, vol. 139, no. 12, pp. 1797–1807, 2013.

[28] H. Zhang, "Study on PPP-BOTDA technology for concrete crack monitoring," *Applied Mechanics and Materials*, vol. 333-335, pp. 1582–1585, 2013.

[29] Z. Zhou, J. He, Y. Huang, and J. Ou, "Experimental investigation of RC beams using BOTDA(R)-FRP-OF," in *Proceedings of 19th International Conference on Optical Fibre Sensors*, vol. 7004, Perth, WA, Australia, May 2008.

[30] T. Guo, A. Li, Y. Song, B. Zhang, Y. Liu, and N. Yu, "Experimental study on strain and deformation monitoring of reinforced concrete structures using PPP-BOTDA," *Science in China Series E: Technological Sciences*, vol. 52, no. 10, pp. 2859–2868, 2009.

[31] C. K. Leung, K. T. Wan, D. Inaudi et al., "Review: optical fiber sensors for civil engineering applications," *Materials and Structures*, vol. 48, no. 4, pp. 871–906, 2013.

[32] M. Imai, R. Nakano, T. Kono et al., "Crack detection application for fiber reinforced concrete using BOCDA-based optical fiber strain sensor," *Journal of Structural Engineering*, vol. 136, no. 8, pp. 1001–1008, 2010.

[33] T. Bao, "Distributed fiber bragg grating sensors for monitoring cracks in concrete structures," in *Proceedings of Thirteenth ASCE Aerospace Division Conference on Engineering, Science, Construction, and Operations in Challenging Environments, and the, NASA/ASCE Workshop on Granular Materials in Space Exploration*, pp. 1390–1399, Pasadena, CA, USA, April 2012.

[34] K. Samrajyam, R. L. Prasad, T. D. Rao, and B. Sobha, "FIBER bragg grating (FBG) sensor for estimation of crack mouth opening displacement (CMOD) in concrete," *Journal of Optics*, vol. 44, no. 4, pp. 346–352, 2015.

[35] J. Mao, F. Xu, Q. Gao et al., "A monitoring method based on FBG for concrete corrosion cracking," *Sensors*, vol. 16, no. 7, 2016.

[36] P. Childs, A. C. Wong, W. K. Terry et al., "Measurement of crack formation in concrete using embedded optical fiber sensors and differential strain analysis," *Measurement Science and Technology*, vol. 19, no. 6, article 065301, 2008.

[37] S. Man, Z. Yong, Y. E. Feng et al., "Comparison research of fiber bragg grating sensors and strain gauges in crack detection," *Sichuan Daxue Xuebao*, vol. 39, no. 6, pp. 45–49, 2007.

[38] Z. Zhou, C. Lan, and J. Ou, "New kind of FBG-based crack (large strain) sensor," in *Proceedings of Smart Structures and Materials 2006: Smart Sensor Monitoring Systems and Applications*, vol. 6167, San Diego, CA, USA, March 2006.

[39] F. Zaidi and K. Krebber, "Advanced hybrid BOFDA/FBG sensor system for simultaneously point-wise and distributed temperature/strain measurements," in *Proceedings of International Conference on Optical Fiber Sensors. International Society for Optics and Photonics*, Santander, Spain, June 2014.

[40] D. Garus, K. Krebber, F. Schliep et al., "Distributed sensing technique based on Brillouin optical-fiber frequency-domain analysis," *Optics Letters*, vol. 21, no. 17, pp. 1402–1404, 1996.

[41] K. O. Hill and G. Meltz, "Fiber Bragg grating technology fundamentals and overview," *Journal of Lightwave Technology*, vol. 15, no. 8, pp. 1263–1276, 1997.

[42] A. D. Kersey, M. A. Davis, H. J. Patrick et al., "Fiber grating sensors," *Journal of Lightwave Technology*, vol. 15, no. 8, pp. 1442–1463, 1997.

[43] H. B. Liu, H. Y. Liu, G. D. Peng et al., "Strain and temperature sensor using a combination of polymer and silica fiber Bragg gratings," *Optics Communications*, vol. 219, no. 1–6, pp. 139–142, 2003.

[44] E. Chehura, S. W. James, R. P. Tatam et al., "Temperature and strain discrimination using a single tilted fiber Bragg grating," *Optics Communications*, vol. 275, no. 2, pp. 344–347, 2007.